Supporting Information

Switching Hydrogen Bonds to Readily Interconvert Two Room-Temperature Long-Term Stable Crystalline Polymorphs in Chiral Molecular Perovskites

Wang-Hua Hu,[a] Wei-Jian Xu,[ab] Qian-Ru Meng,[a] Xue-Wen Zhang,[a] Chun-Ting He,[ac] Wei-Xiong Zhang [*a] and Xiao-Ming Chen[a]

[a] *MOE Key Laboratory of Bioinorganic and Synthetic Chemistry, School of Chemistry, Sun Yat-Sen University, Guangzhou 510275, China.*

[b] *Department of Chemistry & CICECO-Aveiro Institute of Materials, University of Aveiro, 3810-193 Aveiro, Portugal.*

[c] *MOE Key Laboratory of Functional Small Organic Molecule, College of Chemistry and Chemical Engineering, Jiangxi Normal University, Nanchang 330022, China.*

**e-mail: zhangwx6@mail.sysu.edu.cn*

Experimental Details

Materials

Reagents and solvents were commercially available and used without further purification.

Synthesis of 1α

(*R*-$C_5H_{12}NO$)[$CdCl_3$] (**1α**) was synthesized by adding an aqueous solution of $CdCl_2$ (0.228 g, 1.0 mmol) to a stirred aqueous solution of *R*-3-hydroxypiperidine hydrochloride (0.138 g, 1.0 mmol) at room temperature for 5 minutes. The resulted clear solution was allowed to evaporate at room temperature for several days, then the colorless crystals were obtained in a yield of 84%. Elemental analysis, calcd (%) for **1α** ($C_5H_{12}NOCdCl_3$): C, 18.71; N, 4.36; H, 3.77. Found C, 18.68; N, 4.26; H, 3.96.

Synthesis of 1β

(*R*-$C_5H_{12}NO$)[$CdCl_3$] (**1β**) was synthesized by adding $CdCl_2$ (0.456 g, 2.0 mmol) and *R*-3-hydroxypiperidine hydrochloride (0.276 g, 2.0 mmol) in aqueous solution, morpholine hydrochloride (0.123 g, 1.0 mmol) was used as additive agent. The resulted clear solution was allowed to evaporate at room temperature for several days, and the colorless crystals were obtained in a yield of 70%. Elemental analysis, calcd (%) for **1β** ($C_5H_{12}NOCdCl_3$): C, 18.71; N, 4.36; H, 3.77. Found C, 18.69; N, 4.34; H, 3.49.

Syntheses of 2α and 2β

(*S*-$C_5H_{12}NO$)[$CdCl_3$] (**2α** and **2β**) were synthesized by similar methods for **1α** and **1β**, respectively, except *S*-3-hydroxy-piperidine hydrochloride was used in place of *R*-3-hydroxypiperidine hydrochloride. Elemental analysis, calcd (%) for **2α**: C, 18.71; N, 4.36; H, 3.77. Found C, 18.38; N, 4.28; H, 3.17. Elemental analysis, calcd (%) for **2β**: C, 18.71; N, 4.36; H, 3.77. Found C, 18.68; N, 4.34; H, 3.53.

The phase purities were confirmed by matching the PXRD patterns measured at room temperature to the simulated patterns based on the single-crystal structures measured at 25°C (Figure S1 and S2).

Transformation From 1α to 1β

The powder samples of **1α** (5.0 mg) were heated up to 200°C in a thermogravimetric (TG) apparatus with a heating rate of 5°C min^{-1} under N_2 atmosphere, and kept for 10 minutes at 200°C, then were naturally cooled down to room temperature.

Transformation From 1β to 1α

The powder samples of **1β** were put into tablet molds with diameters of 13 mm and then pressed by putting weight of 20–65 kg on the top for applying pressures of 1.5–4.8 MPa, and were put into tablet moulds with diameters of 5 mm and then pressed by tablet compression machine for applying pressures of 1.0–5.0 GPa, respectively. After applying the pressure for 10 minutes at room temperature, the phases of the pressed tablets were checked by PXRD patterns.

Transformation From 1δ to 1α

The sample of **1δ** obtained by heating the powder sample of **1β** (5.0 mg) to 220°C in a TG apparatus with a heating rate of 5°C min^{-1} was thrown into liquid N_2 immediately. After naturally warming up to room temperature, the obtained sample of **1α** was checked by PXRD patterns.

Single-Crystal X-ray Diffraction

Single-crystal X-ray diffraction data were collected on a Rigaku XtaLAB P300DS with Mo-Kα radiation (λ = 0.71073 Å) for **1α**, **2α**, and **2β** at 25°C, on a Rigaku R-AXIS SPIDER IP diffractometer with Mo Kα radiation (λ = 0.71073 Å) for **1β** at 25°C, and on a Rigaku SuperNova diffractometer for **1δ** and **2δ** with Cu-Kα radiation (λ = 1.54184 Å) at 177°C. Data processing including empirical absorption correction was finished with the *Crystalclear* software package (Rigaku, 2005). The crystal structures were solved with direct methods and then refined by full-matrix least-squares refinements on F^2 with the SHELX software package.[S1, S2] The atomic displace parameters were refined anisotropically for all non-hydrogen atoms. The positions of all hydrogen atoms were generated geometrically. The crystal structure packing views were drawn with DIAMOND software. Detailed crystallographic data and structure refinement parameters are listed in Table S1. CCDC numbers: 1886374-1886377, 1901972 and 1901973.

Computational Details

Density functional theory (DFT) calculations were carried out by employing a Dmol^3 module in Materials Studio 5.5 package. The initial structures are taken directly from the single-crystal X-ray data of **1α** and **1β** at 25°C, which were geometrically optimized with the cell parameters fixed, by using the generalized gradient approximation (GGA) with Perdew-Becke-Ernzerhof (PBE) exchange-correlation function. The double numerical plus polarization (DNP) basis set was used for the non-metal atoms. An accurate DFT Semi-core Pseudopots (DSPP) was employed for the cadmium atom. The total energies of the final optimized structures were used for the comparison.

Powder X-ray Diffraction (PXRD)

The PXRD patterns were collected in the range of 2θ = 5°–70° with a step size of 0.02°, performed on a Bruker D8 ADVANCE X-ray powder diffractometer (Cu-Kα, λ = 1.54056 Å) at 25–205°C.

Thermal Measurements

Differential scanning calorimeter (DSC) measurements were carried out with a TA DSC Q2000 instrument by heating and cooling runs with a rate of 5°C min^{-1}. The sample was loaded into an aluminum pan under flowing nitrogen at atmospheric pressure. Thermogravimetric (TG) analysis was conducted using a TA Q50 system with a heating rate of 10°C min^{-1} under the nitrogen atmosphere.

Dielectric Constant Measurement

A pressed-powder pellet sample of **1α** pasted with silver conducting glue as the electrodes was used in dielectric measurements, pellets with 12 mm in diameter and 0.2 mm thick were prepared by pressing microcrystal samples at 433 MPa. The temperature-dependent dielectric constant was measured on a TH2828A Impedance Analyzer at different frequencies from 2.5 kHz to 1 MHz, with the AC field amplitude of 1 V, and a temperature heating/cooling rate of 3°C min^{-1} in a Mercury iTC cryogenic environment controller of Oxford Instrument.

Second Harmonic Generation (SHG) Measurement

Variable-temperature SHG experiment was carried out by powder samples on an XPL 1064-200 Instruments, using an Nd:YAG laser (1064 nm) staring on a powder sample of **1α**.

Elemental Analyses

Elemental (C, H, and N) analyses were performed on an Elementar Vario EL Cube elemental analyzer.

Fourier Transform Infrared (FT-IR) Spectra Measurement

FT-IR spectra were obtained from KBr pellets on a Bruker Tensor 27 FT-IR spectrometer in the 600–4000 cm^{-1} region in a Mercury iTC cryogenic environment controller of Oxford Instrument.

Hirshfeld Surface Analysis

Hirshfeld surfaces and 2D fingerprint plots were produced using CrystalExplorer 17 based on the results of single-crystal structures, all bond lengths to hydrogen atoms were normalized to typical neutron bond lengths (*i.e.*, C–H = 1.083 Å, O–H =0.983 Å, N–H = 1.009 Å) when calculating the Hirshfeld surfaces by CrystalExplorer. [S3-S5]

Table S1. Crystallographic parameters for **1α**, **1β**, **2α**, **2β** at 25°C, **1δ**, **2δ** at 177°C.

	1α	**1β**	**1δ**	**2α**	**2β**	**2δ**
Chemical formula		(R-$C_5H_{12}NO$)[$CdCl_3$]			(S-$C_5H_{12}NO$)[$CdCl_3$]	
Formula weight	320.92	320.92	320.92	320.92	320.92	320.92
T / °C	25(2)	25(2)	177(2)	25(2)	25(2)	177(2)
Crystal system	orthorhombic	orthorhombic	hexagonal	orthorhombic	orthorhombic	hexagonal
Space group	$P2_12_12_1$	$P2_12_12_1$	$P6_322$	$P2_12_12_1$	$P2_12_12_1$	$P6_322$
a / Å	10.1144(3)	9.3179(6)	9.481(4)	10.1085(3)	9.2835(3)	9.448(1)
b / Å	14.5189(5)	15.543(1)	9.481(4)	14.5205(4)	15.4731(5)	9.448(1)
c / Å	6.7661(2)	6.8068(5)	6.755(2)	6.7609(2)	6.7890(3)	6.7395(5)
V / Å^3	993.60(5)	985.8(1)	525.8(3)	992.37(5)	975.20(6)	521.0(1)
Z	4	4	2	4	4	2
ρ_{calc} / (g cm^{-3})	2.145	2.162	2.027	2.148	2.186	2.046
μ / mm^{-1}	2.951	2.975	23.261	2.955	3.007	23.477
Reflns. collected	6118	13016	2090	4760	8071	1798
Independent reflns.	1950	2235	285	1931	2295	165
R_1[a], wR_2[b] [$I \geq 2\sigma(I)$]	0.0400, 0.0929	0.0298, 0.0778	0.0408, 0.0979	0.0286, 0.0731	0.0561, 0.1538	0.0307,0.0796
R_1[a], wR_2[b] (all data)	0.0424, 0.1033	0.0307, 0.0783	0.0675, 0.1197	0.0359, 0.0760	0.0668, 0.1936	0.0369, 0.0857
Flack	-0.01(7)	0.03(6)	0.1(7)	-0.03(4)	0.1(2)	-0.3(4)
GOF on F^2	1.173	1.138	1.078	1.105	1.132	1.208
CCDC numbers	1886374	1886375	1901972	1886376	1886377	1901973

[a] $R_1 = \sum||F_o|-|F_c||/\sum|F_o|$;

[b] $wR_2 = [\sum w(F_o^2 - F_c^2)^2/\sum w(F_o^2)^2]^{1/2}$.

Table S2. Selected bond distances (Å), atomic distances (Å) and bond angles (°).

	1α	**1β**	**1δ**	**2α**	**2β**	**2δ**
Chemical formula		(R-$C_5H_{12}NO$)[$CdCl_3$]			(S-$C_5H_{12}NO$)[$CdCl_3$]	
T / °C	25(2)	25(2)	177(2)	25(2)	25(2)	177(2)
Cd−Cl	2.6145(9)-2.6671(7)	2.6032(9)-2.6868(9)	2.645(3)	2.6135(9)-2.667(8)	2.592(3)-2.679(2)	2.638(4)
cis Cl−Cd−Cl	80.69(3)-100.68(4)	81.55(3)-99.61(3)	83.59(7)-96.41(7)	80.66(3)-100.67(4)	81.67(8)-99.75(8)	83.6(1)-96.4(1)
trans Cl−Cd−Cl	175.20(3)-176.53(1)	178.52(1)-178.67(3)	180.0	175.15(3)-176.55(1)	178.57(3)-178.64(8)	180.0
Cd···Cd (inter-chain)	8.8387(4)-10.1144(5)	9.0135(6)- 9.3179(7)	9.481(4)	8.8377(5)-10.1085(5)	8.976(1)-9.284(1)	9.448(1)
Cd···Cd (intra-chain)	3.3868(1)	3.4041(3)	3.3775(8)	3.3842(1)	3.3952(2)	3.3697(2)
Cd−Cd−Cd	174.59(2)	177.64(1)	180.0	174.60(2)	177.71(4)	180
Cd−Cl−Cd	79.11(2)-80.41(2)	79.30(2)-81.31(2)	79.37(9)	79.07(2)-80.41(3)	79.27(7)-81.46(7)	79.4(1)

Table S3. Hydrogen bonds for **1α** and **1β** at 25°C.

D	H	A	*d*(D-H)/Å	*d*(H-A)/Å	*d*(D-A)/Å	D-H-A/°
1α						
N1	H1B	O1[a]	0.90	2.27	3.038(5)	143.2
N1	H1A	Cl2	0.90	2.63	3.483(3)	157.4
O1	H1	Cl1[b]	0.82	2.40	3.137(3)	150.7
1β						
N1	H1A	O1[c]	0.90	2.16	2.982(5)	150.7
O1	H1	Cl2	0.82	2.40	3.193(4)	162.6
2α						
N1	H1B	O1[d]	0.900	2.273	3.038(5)	142.71
N1	H1A	Cl2[e]	0.900	2.628	3.475(3)	157.23
O1	H1	Cl3[f]	0.820	2.401	3.137(3)	149.81
2β						
N1	H1B	O1[g]	0.900	2.127	2.955(5)	152.41
O1	H1	Cl2[h]	0.820	2.417	3.186(4)	156.44

[a] (-*x*+3/2, -*y*+1, *z*-1/2); [b] (-*x*+3/2, -*y*+1, *z*+1/2); [c] (*x*+1/2, -*y*+1/2, -*z*+2); [d] (-*x*+3/2, -*y*+1, *z*-1/2); [e] (*x*+1, *y*, *z*); [f] (-*x*+1/2, -*y*+1, *z*+1/2); [g] (*x*-1/2, -*y*+1/2, -*z*+2); [h] (*x*+1, *y*, *z*).

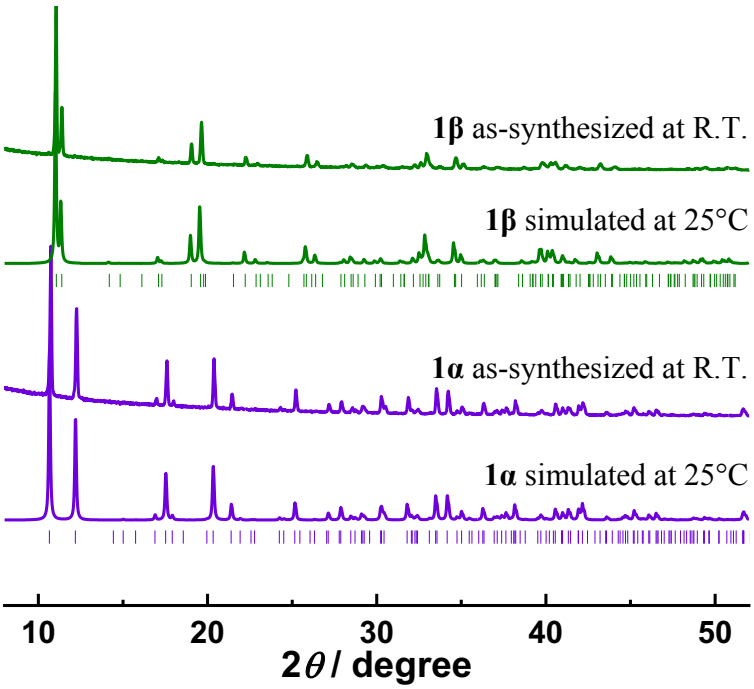

Figure S1. The simulated and experimental PXRD patterns of **1α** and **1β** at room temperature.

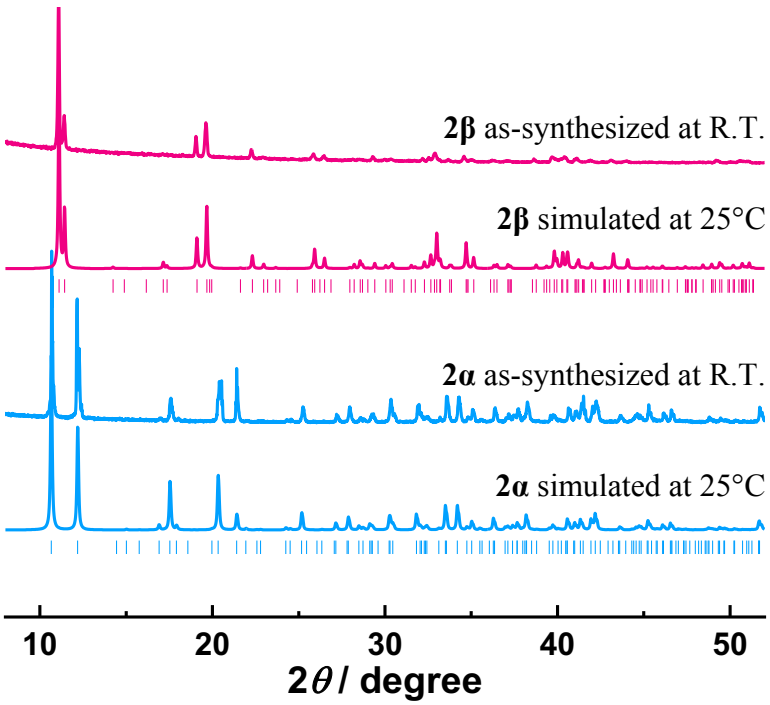

Figure S2. The simulated and experimental PXRD patterns of **2α** and **2β** at room temperature.

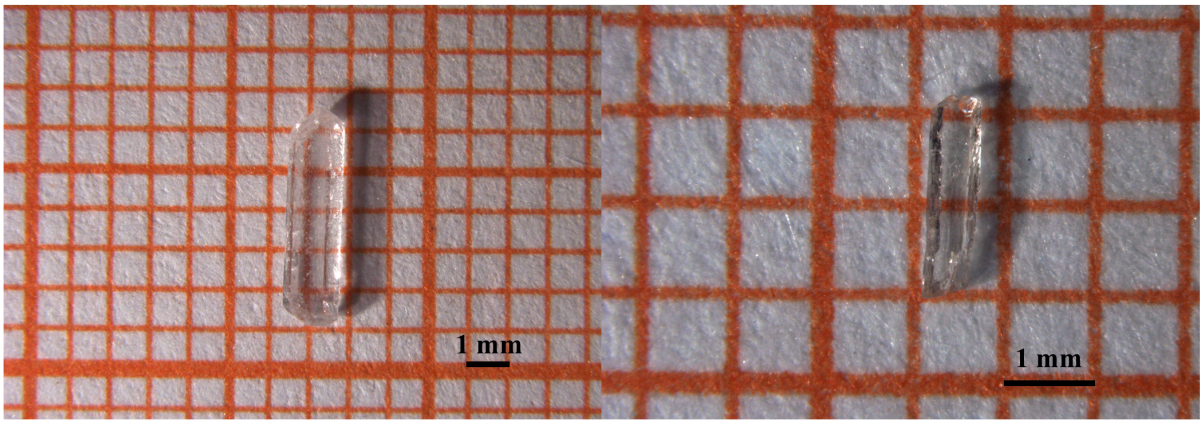

Figure S3. Single crystals of **1α** (left) and **1β** (right).

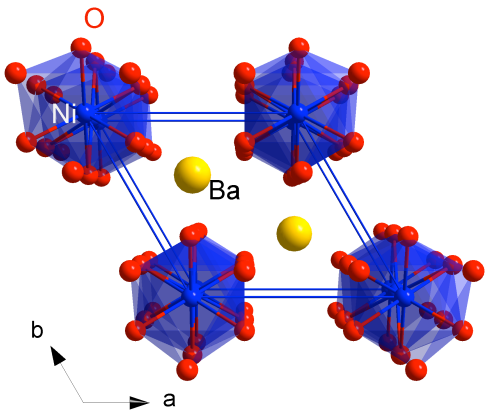

Figure S4. Structure of hexagonal inorganic perovskite oxides, as exemplified by $BaNiO_3$.

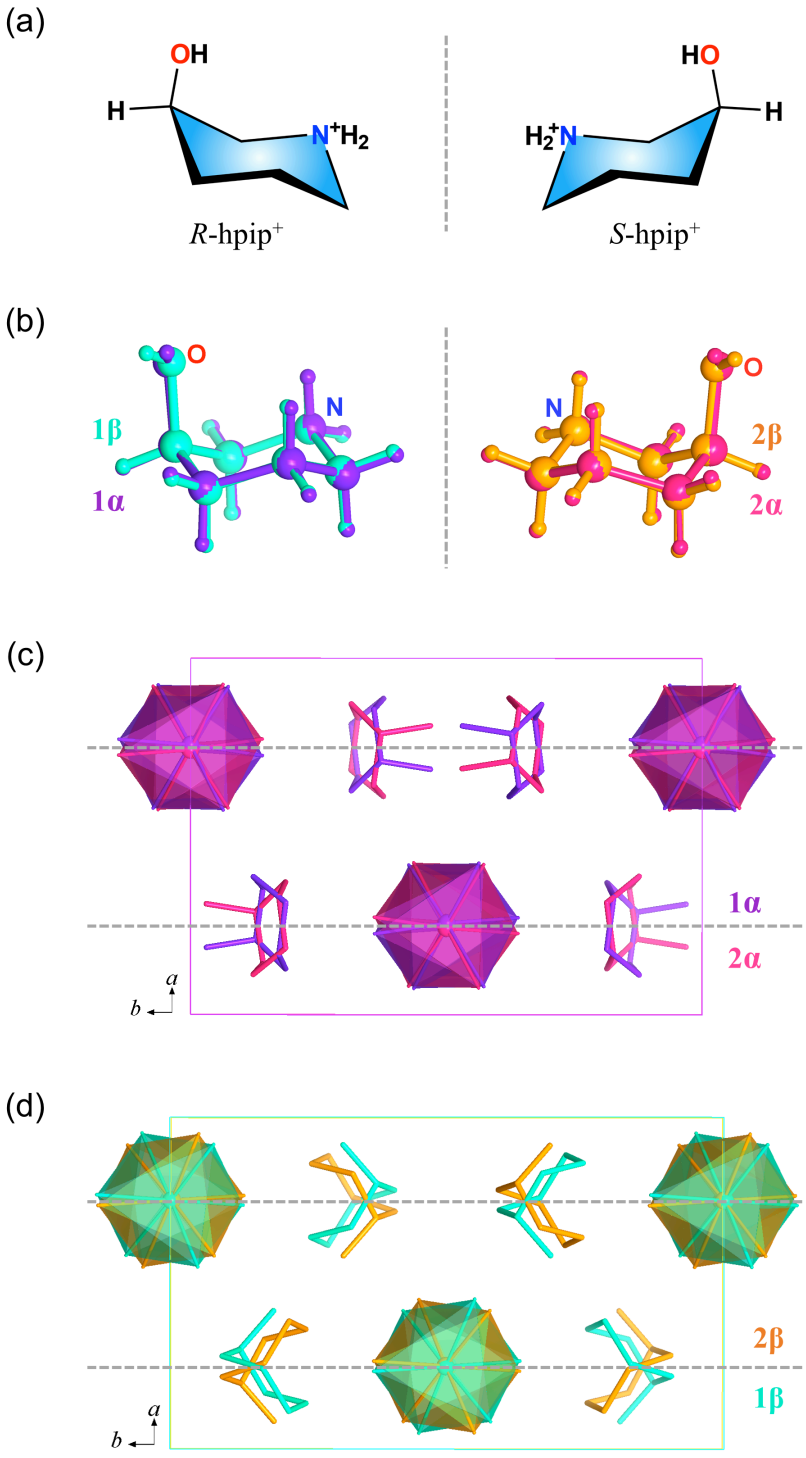

Figure S5. (a) The structure of *R*-hpip$^+$ and *S*-hpip$^+$ cations. (b) Overlap of the homochiral organic cations in **1α** (purple) and **1β** (cyan), and those in **2α** (rose red) and **2β** (orange). (c) The enantiomorphic relationship between **1α** and **2α**, all hydrogen atoms are omitted for clarity. (d) The enantiomorphic relationship between **1β** and **2β**, all hydrogen atoms are omitted for clarity.

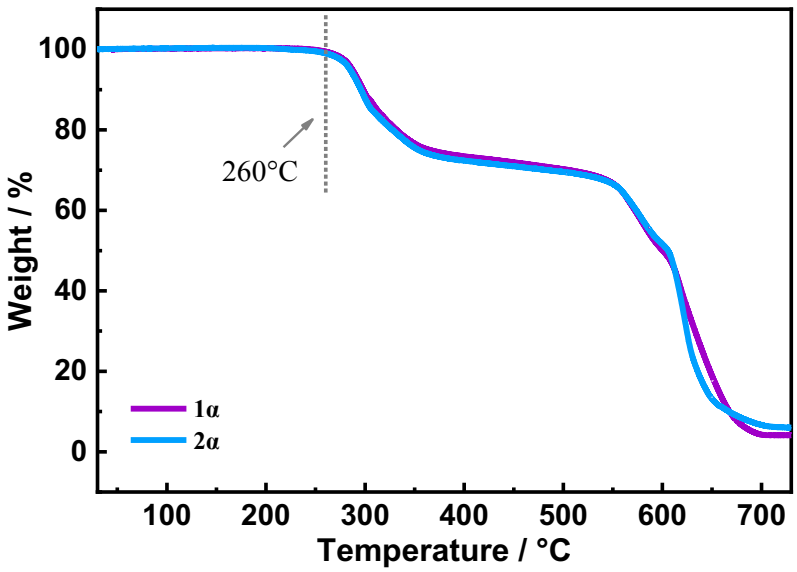

Figure S6. TG curves for **1α** and **2α**.

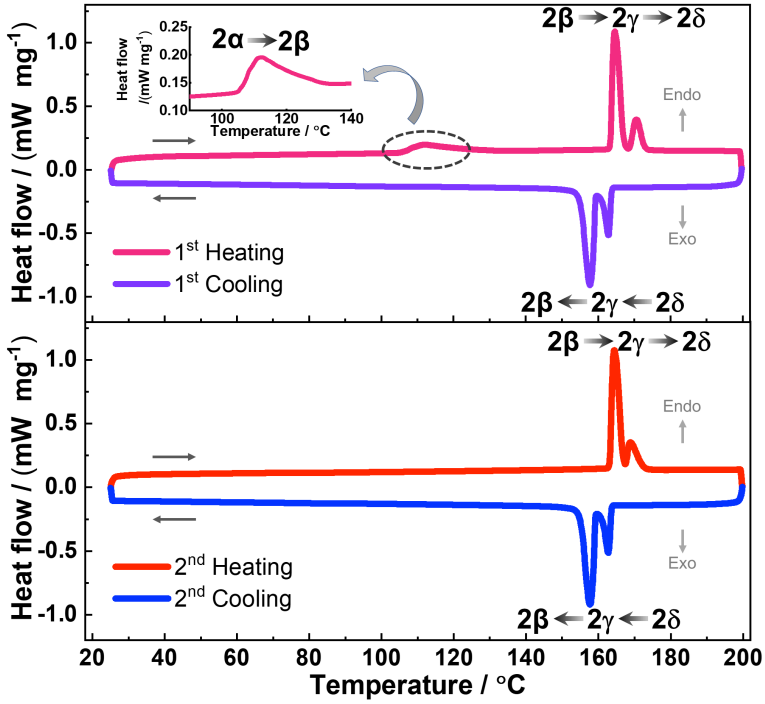

Figure S7. DSC curves for **2** with two heating-cooling runs starting from **2α**.

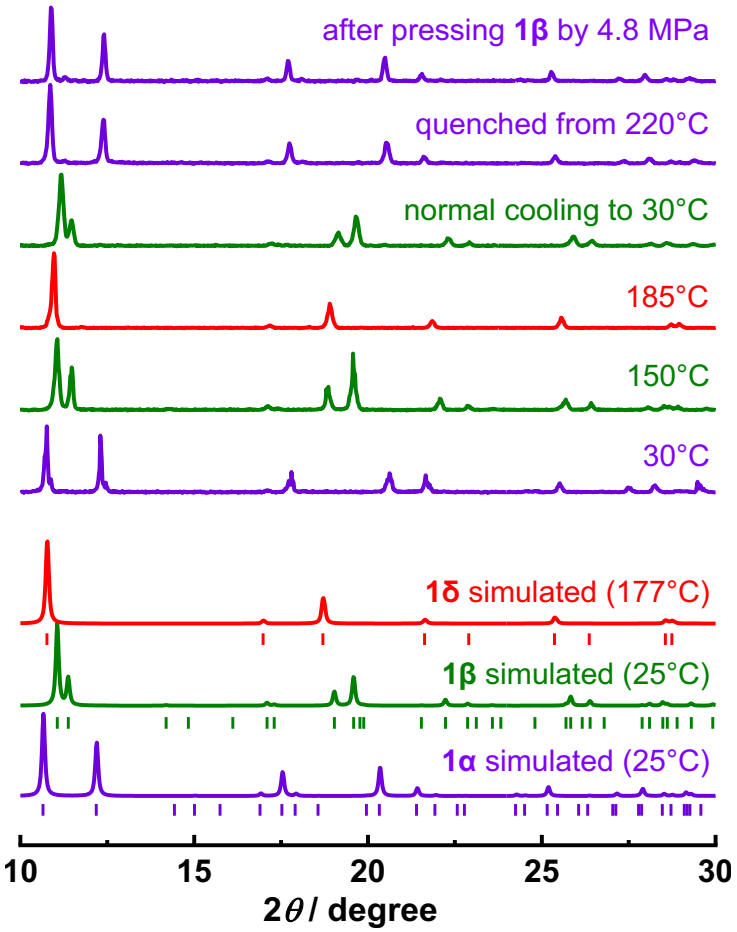

Figure S8. Simulated PXRD patterns of **1α**, **1β**, **1δ**, and experimental PXRD patterns for *in-situ* variable-temperature measurement starting from **1α** sample at 30°C, 150°C, 185°C and cooling back to 30°C, and for the samples quenched from 220°C and pressed **1β** under 4.8 MPa.

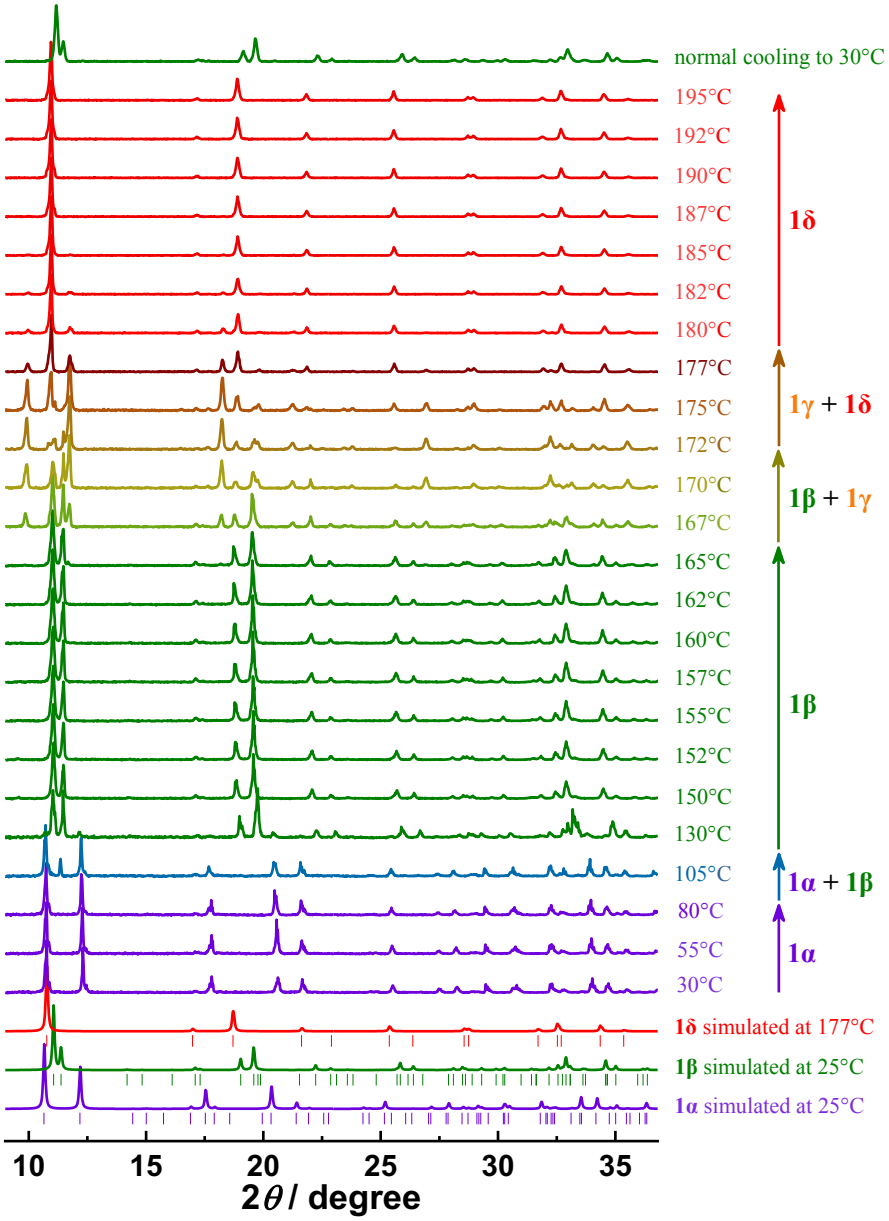

Figure S9. A heating-cooling run of *in situ* variable-temperature PXRD patterns measured starting from the **1α** form.

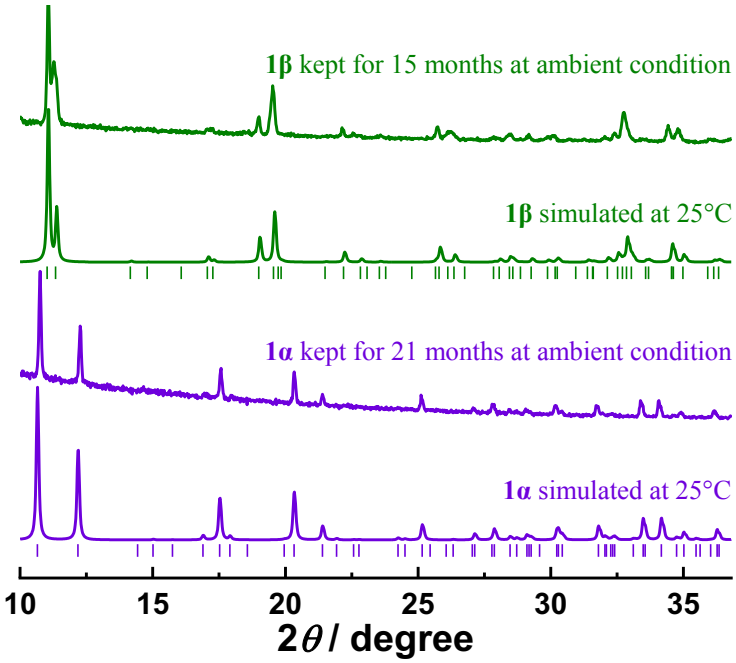

Figure S10. The simulated and experimental PXRD patterns of **1α** and **1β** kept at ambient temperature and pressure for 21 and 15 months, respectively.

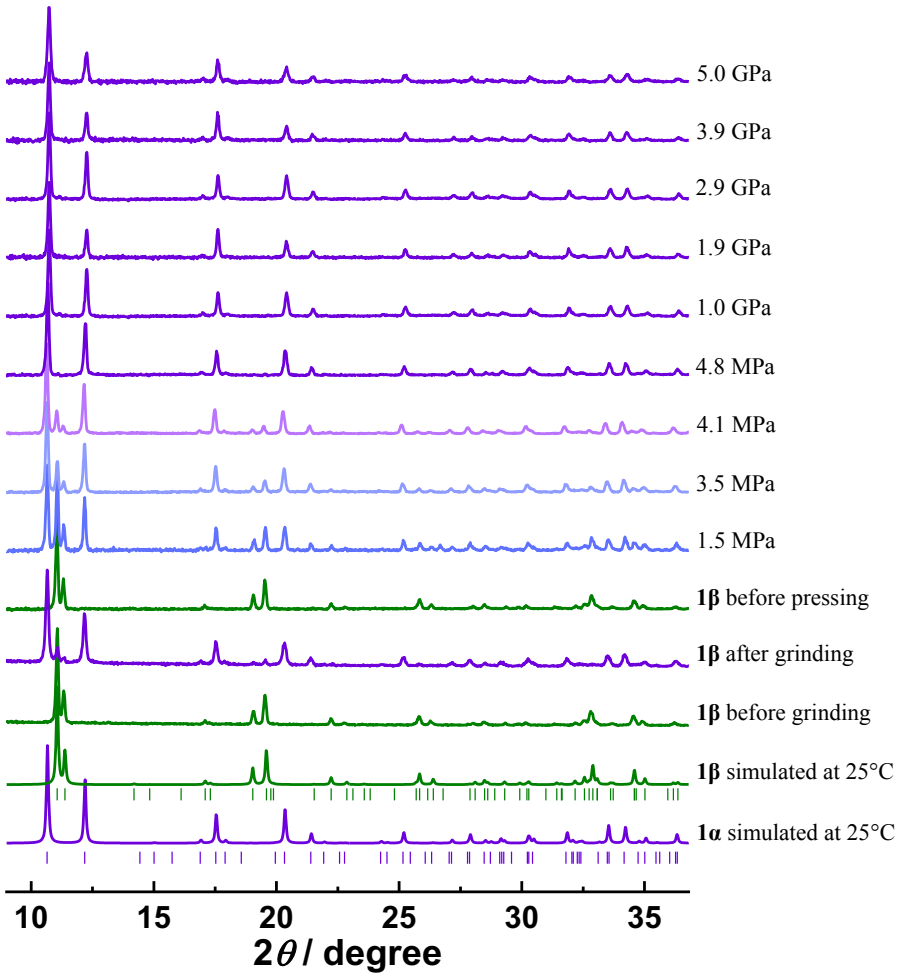

Figure S11. The PXRD patterns measured at ambient pressure for the samples after grinding **1β** sample by hand for 5 minutes, and pressing **1β** sample by applying different external pressures for 10 minutes.

To check the repeatability of the **1α** and **1β** forms could be obtained by quenching and normal cooling of a high-temperature phase **1δ**, respectively, two cycles were performed by heating **1α** to 220°C and normal cooling to room temperature (*i.e.*, yielding **1β**) and then heated again to 220°C and quenched by liquid nitrogen, then back to room temperature (*i.e.*, yielding **1α**). All the PXRD patterns were measured for the resulted samples at ambient temperature and ambient pressure.

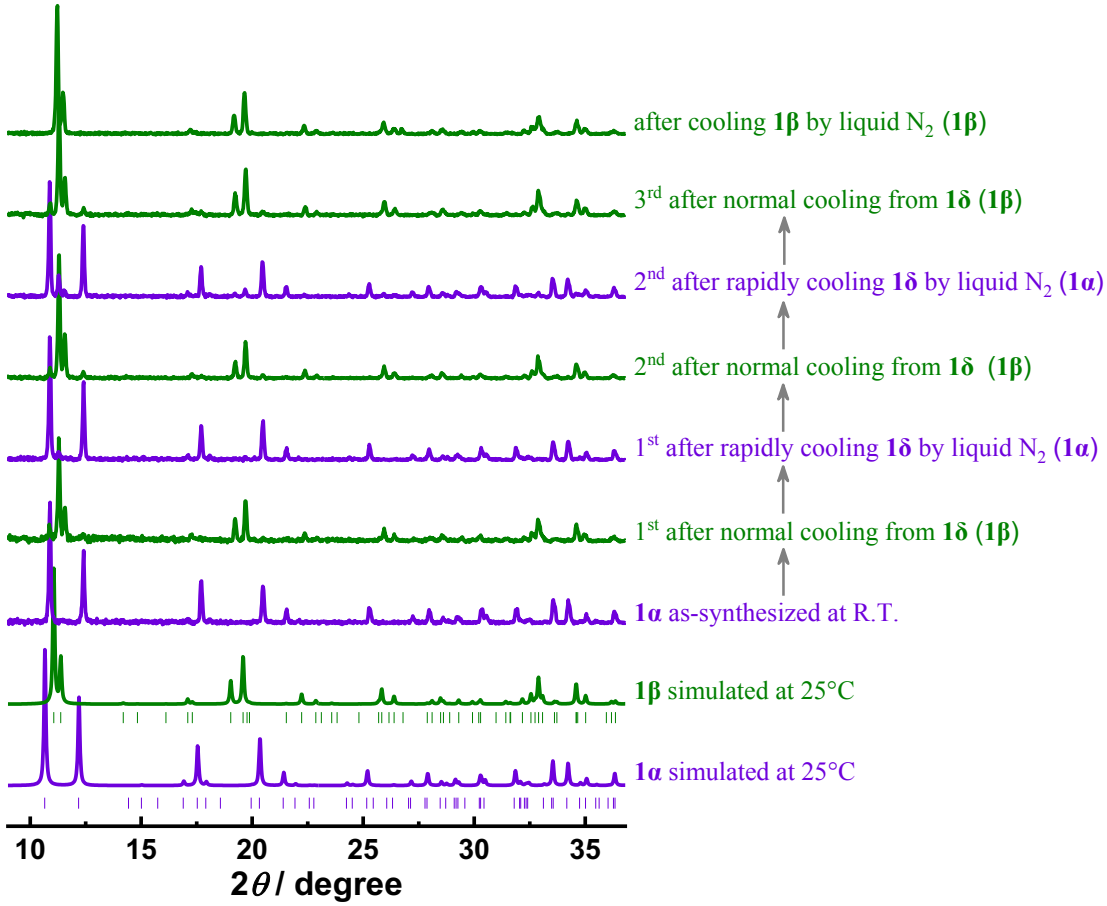

Figure S12. Repeatability of the **1α** and **1β** forms obtained by quenching and normal cooling of a high-temperature phase **1δ**.

To check the repeatability of the heat-and-pressure-induced phase transition between the **1α** and **1β** forms, four heat-and-pressure cycles were performed by heating **1α** to 220°C and normal cooling to room temperature (*i.e.*, yielding **1β**) and then applying external pressure of 5.0 GPa on **1β** at room temperature for 10 minutes (*i.e.*, yielding **1α**). All the PXRD patterns were measured for the resulted samples at ambient temperature and ambient pressure.

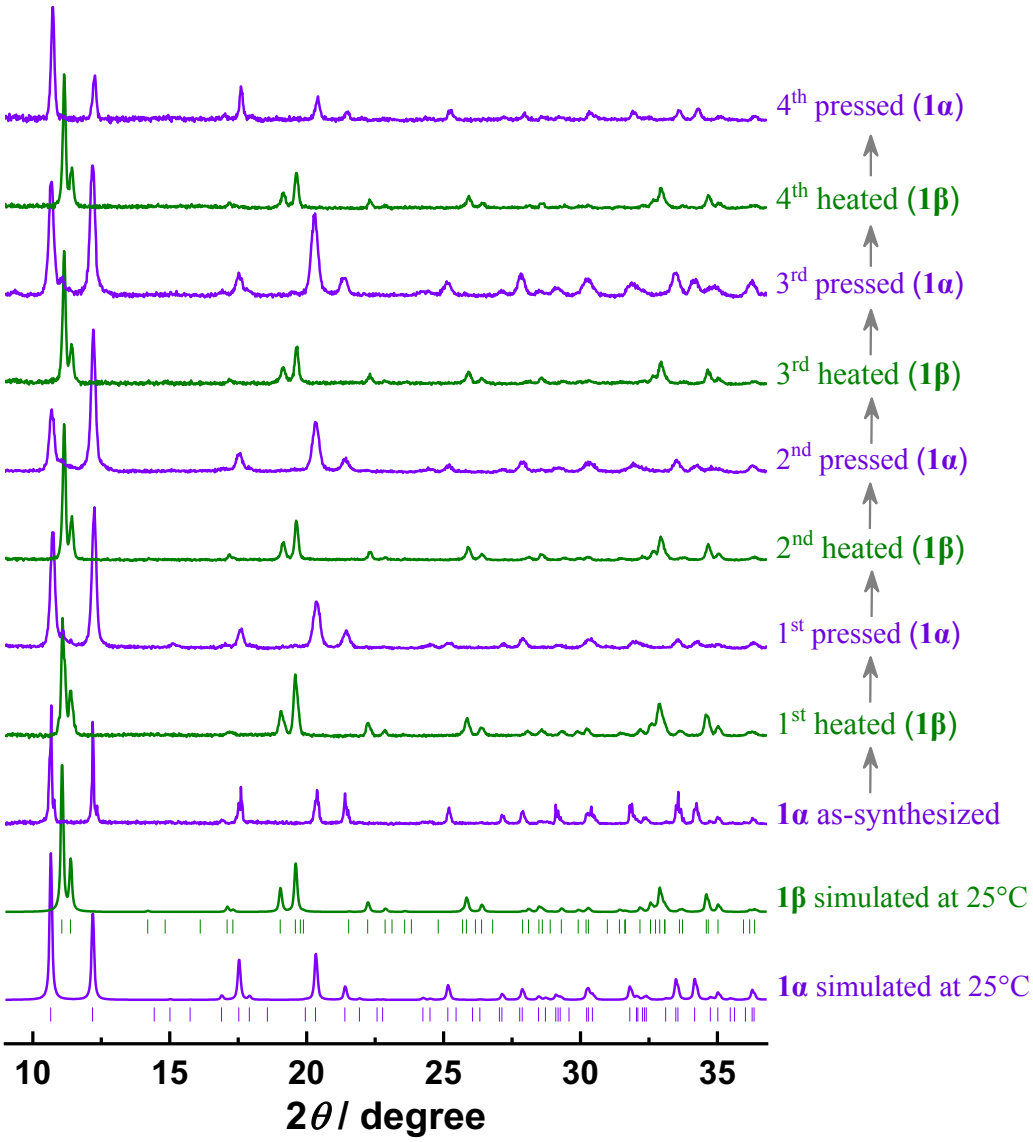

Figure S13. Repeatability of the heat-and-pressure-induced phase transition between the **1α** and **1β**.

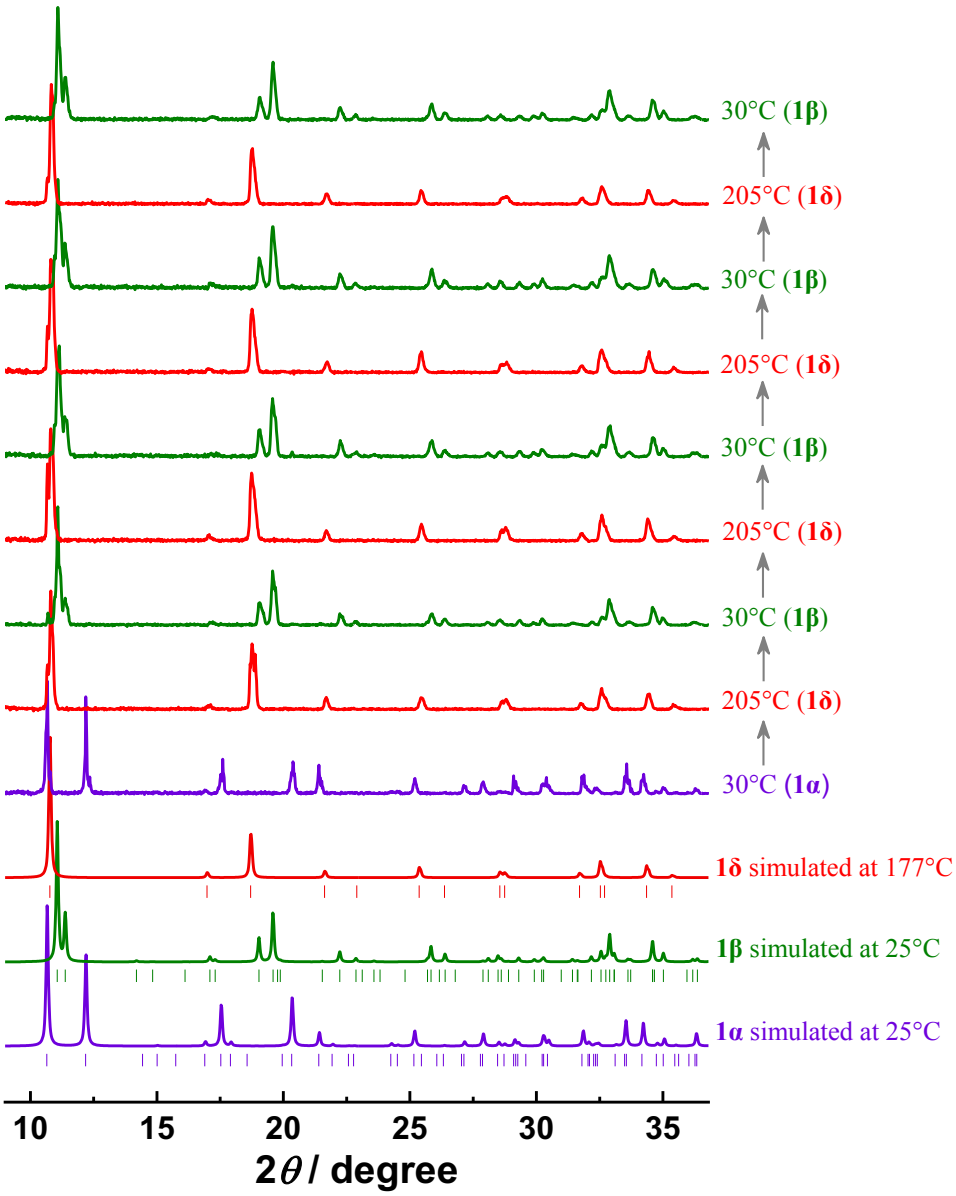

Figure S14. Variable-temperature PXRD patterns of four heating-cooling cycles starting from **1α**, confirming the reversible thermal-induced transitions for **1**.

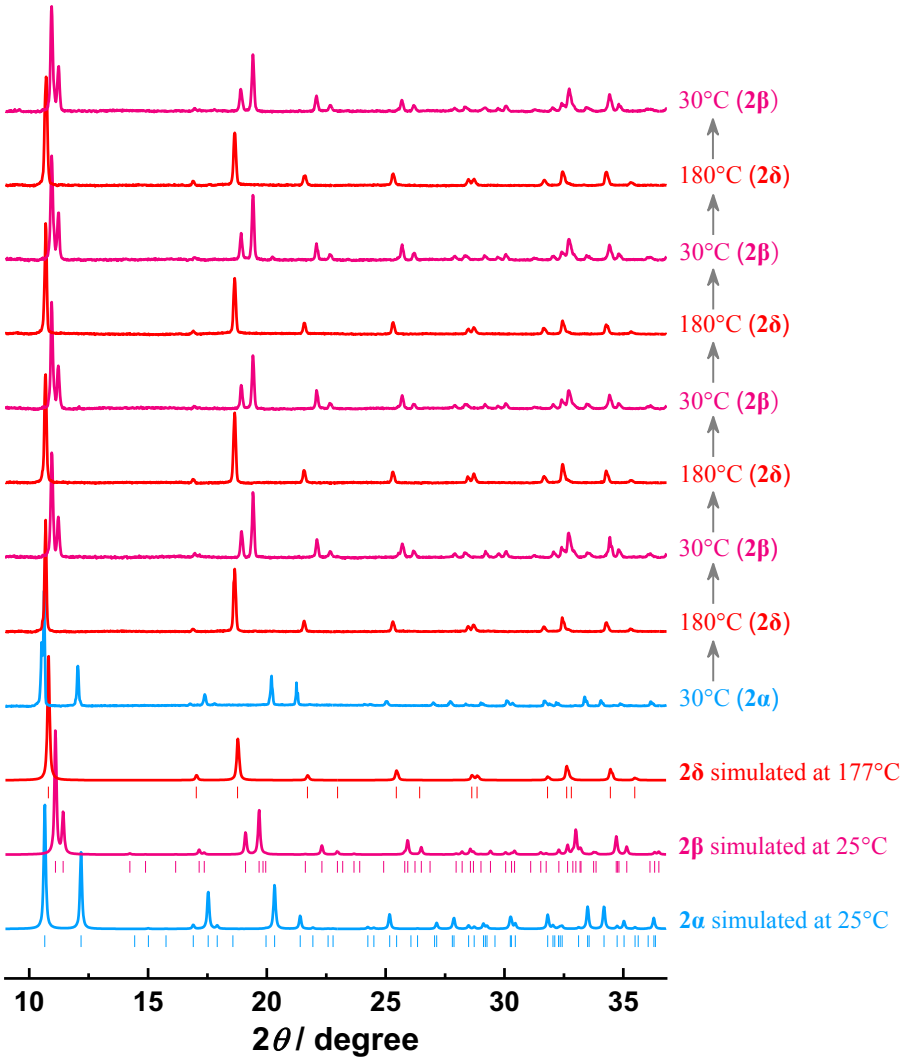

Figure S15. Variable-temperature PXRD patterns of four heating-cooling cycles starting from **2α**, confirming the reversible thermal-induced transitions for **2**.

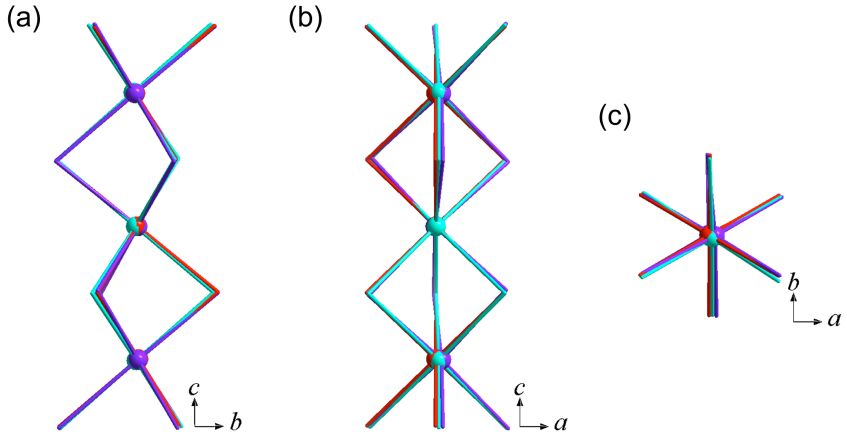

Figure S16. Overlapping the inorganic chains in **1α** (purple), **1β** (cyan) and **1δ** (red) viewed along the *a*-, *b*-, and *c*-axis in space group $P2_12_12_1$, respectively.

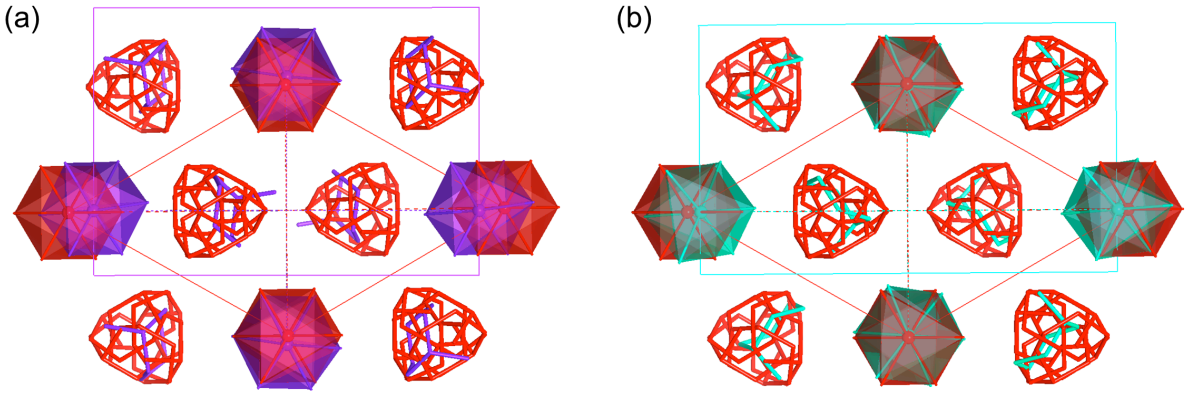

Figure S17. Overlap of unit cells of **1δ** (red) with (a) **1α** (purple) and (b) **1β** (cyan), respectively. All hydrogen atoms are omitted for clarity.

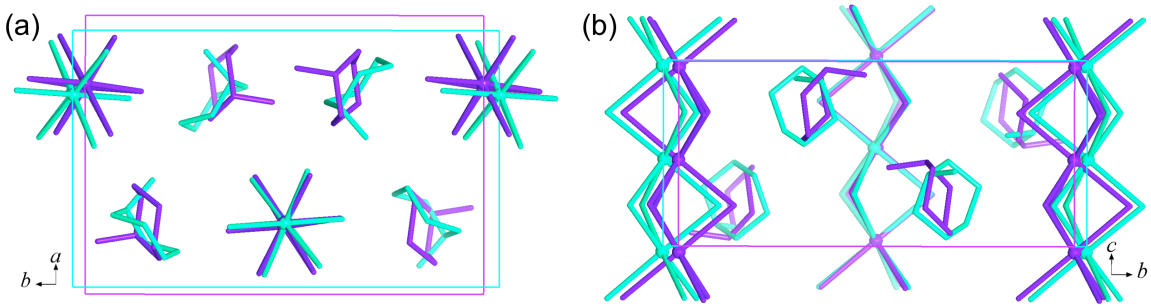

Figure S18. Overlap of unit cells of **1α** (purple) and **1β** (cyan) viewing along the *c*-axis (a) and *a*-axis (b). All hydrogen atoms are omitted for clarity.

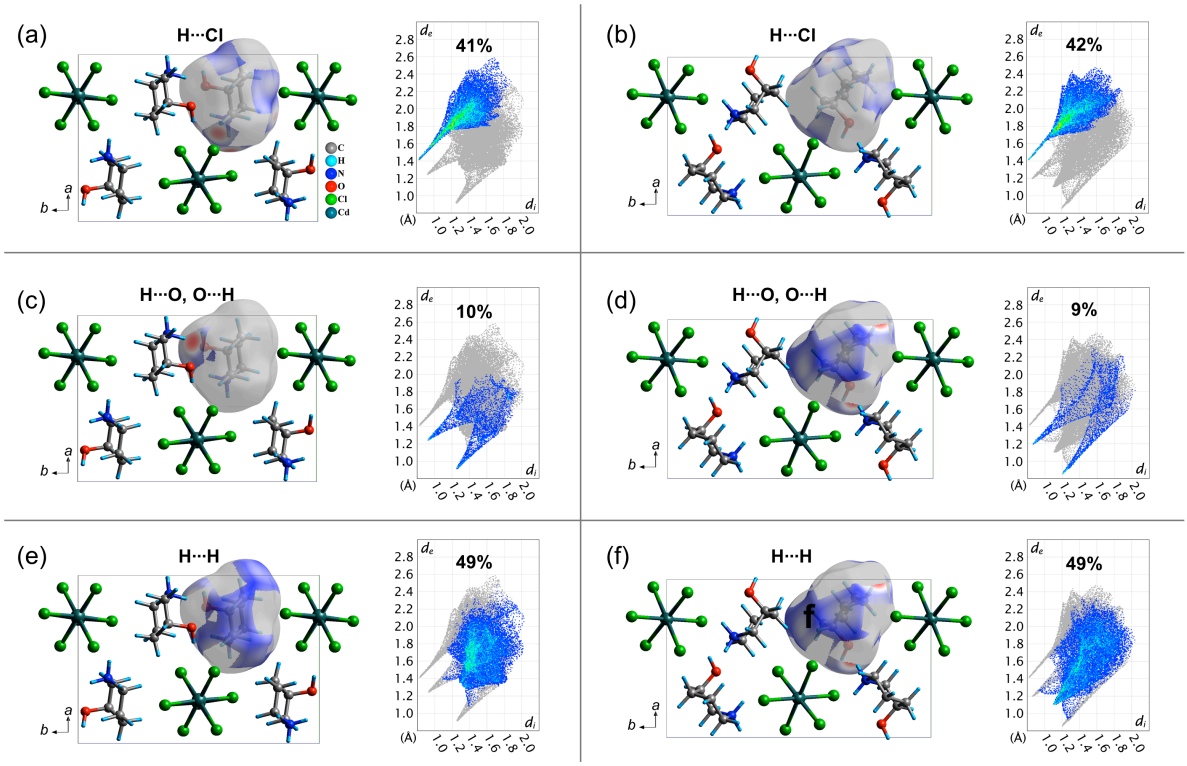

Figure S19. Hirshfeld surface for the organic cations in **1α** (a, c, e) and **1β** (b, d, f) at 25°C, for the specific short contacts of H···Cl (a, b), H···O and O···H (c, d), H···H (e, f), with d_i and d_e ranging from -0.4 to 1.1 Å.

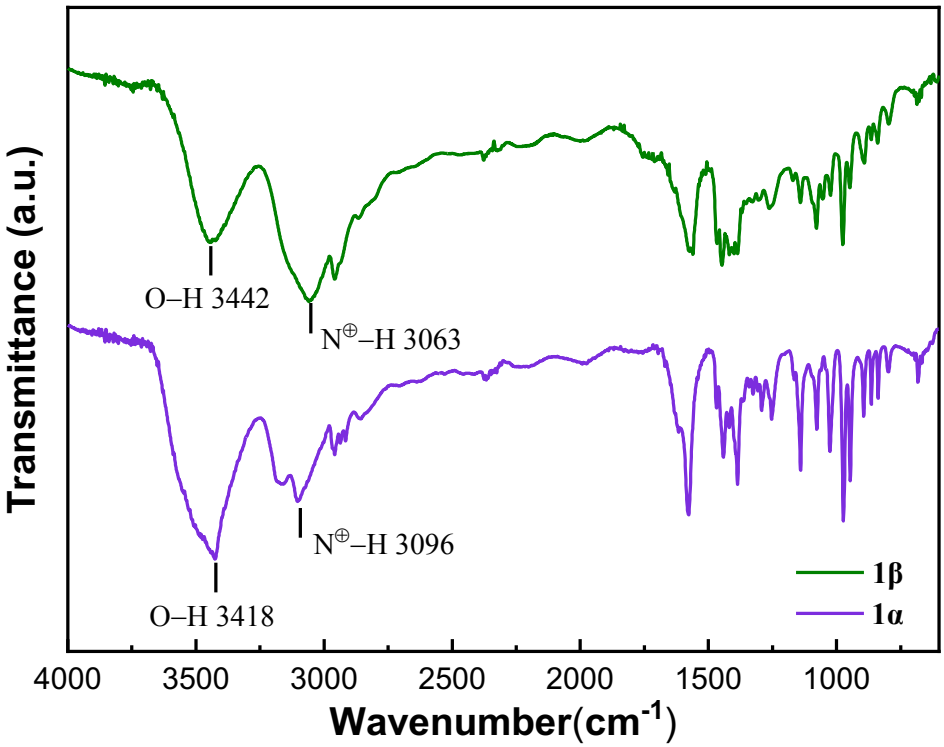

Figure S20. FTIR spectra of **1α** and **1β** (obtained by *in situ* heating **1α** up to 177°C and then normally cooled) at 25°C.

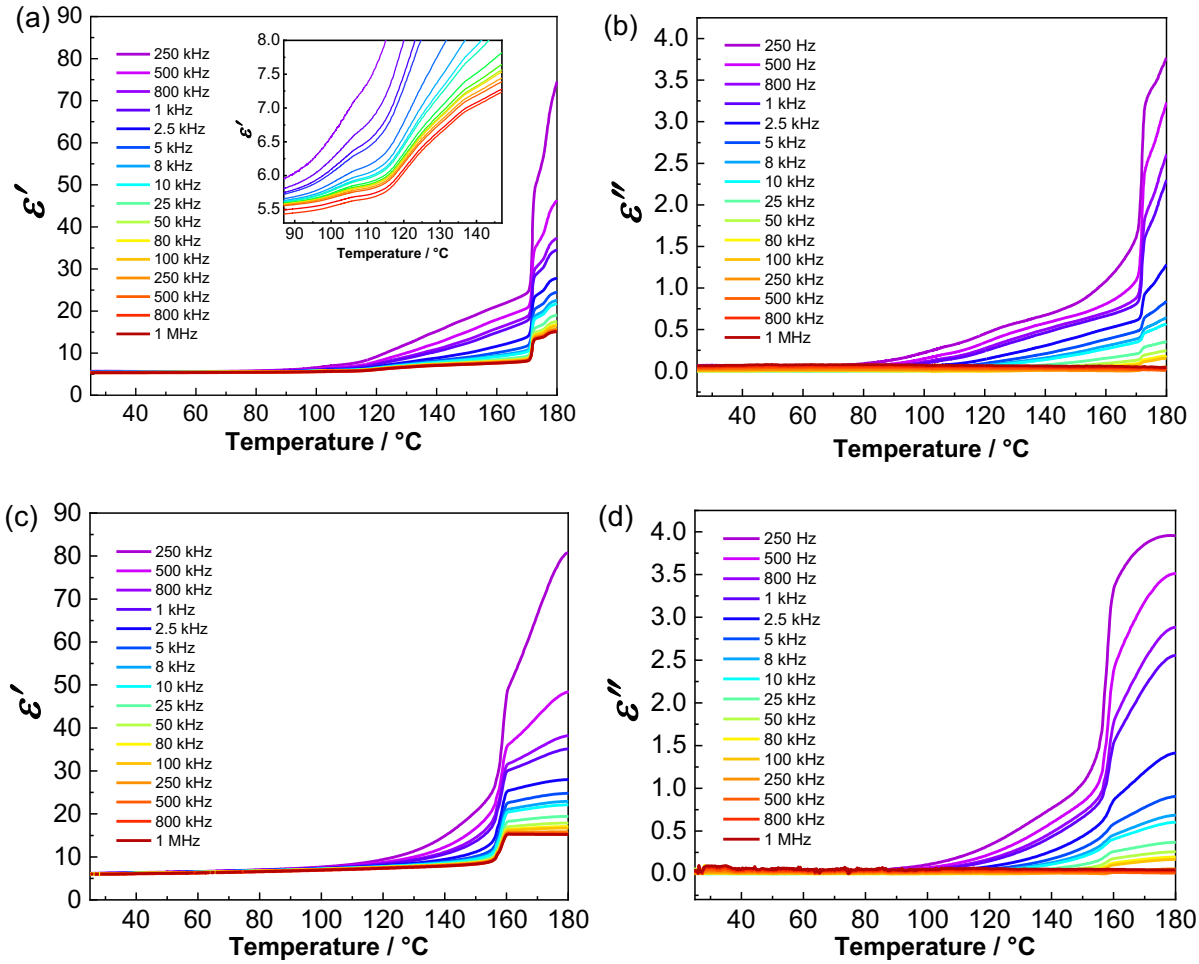

Figure S21. Real (a, c) and imaginary (b, d) part of the dielectric constants on a pelleted sample of **1** at different frequencies from 2.5 kHz to 1 MHz on heating (a, b) and cooling (c, d) processes measured starting from **1α**. Inset (a): Plot of ε' vs. temperature of heating mode from 87°C to 147°C for **1α**.

References

[S1] O. V. Dolomanov, L. J. Bourhis, R. J. Gildea, J. A. K. Howard and H. Puschmann, *J. Appl. Cryst.,* 2009, **42**, 339-341.

[S2] G. Sheldrick, *Acta Cryst. A*, 2008, **64**, 112-122.

[S3] M. J. Turner, J. J. McKinnon, S. K. Wolff, D. J. Grimwood, P. R. Spackman, D. Jayatilaka and M. A. Spackman, CrystalExplorer17 (2017). University of Western Australia.

[S4] M. A. Spackman and J. J. McKinnon, *CrystEngComm*, 2002, **4**, 378-392.

[S5] J. J. McKinnon, D. Jayatilaka and M. A. Spackman, *Chem. Commun.,* 2007, **37**, 3814-3816.